Coordination between CCR7- and CCR9-mediated chemokine signals in prevascular fetal thymus colonization

Cunlan Liu, Fumi Saito, Zhijie Liu, Yu Lei, Shoji Uehara, Paul Love, Martin Lipp, Shunzo Kondo, Nancy Manley, and Yousuke Takahama

Thymus seeding by T-lymphoid progenitor cells is a prerequisite for T-cell development. However, molecules guiding thymus colonization and their roles before and after thymus vascularization are unclear. Here we show that mice doubly deficient for chemokine receptors CCR7 and CCR9 were defective specifically in fetal thymus colonization before, but not after, thymus vascularization. The defective prevascular fetal thymus colonization was followed by selective loss of the first wave of T-cell development generating epidermal Vγ3$^+$ γδ T cells. Unexpectedly, CCL21, a CCR7 ligand, was expressed not by Foxn1-dependent thymic primordium but by Gcm2-dependent parathyroid primordium, whereas CCL25, a CCR9 ligand, was predominantly expressed by Foxn1-dependent thymic primordium, revealing the role of the adjacent parathyroid in guiding fetal thymus colonization. These results indicate coordination between Gcm2-dependent parathyroid and Foxn1-dependent thymic primordia in establishing CCL21/CCR7- and CCL25/CCR9-mediated chemokine guidance essential for prevascular fetal thymus colonization. (Blood. 2006;108: 2531-2539)

Introduction

Seeding of the thymus by hematopoietic stem cell–derived T-lymphoid progenitor cells is essential for the generation of T lymphocytes in the thymus. T lymphopoiesis in the thymus is initiated on the embryonic colonization by T-lymphoid progenitor cells of the thymic primordium that is generated at the third pharyngeal pouch endoderm. The colonization of the fetal thymus begins at gestation week 7 to 8 in humans and at embryonic day 11.5 (E11.5) in mice, before the development of vasculatures in the thymus.[1,2] It was suggested that chemotactic guidance regulates the recruitment of T-lymphoid progenitor cells by the fetal thymus.[3,4] However, the molecules that guide fetal thymus colonization and their roles before and after the thymus vascularization have not been established.

It was shown that the fetal thymus produces several chemokines including CCL21, CCL25, and CXCL12.[5,6] We recently reported that the in vitro attraction of T-lymphoid progenitor cells to the fetal thymus rudiment is mediated by G-protein–dependent chemotactic signals and is impaired by neutralizing antibodies specific for CCL21 and CCL25 but not by antibodies specific for CXCL12, suggesting the involvement of CCL21 and CCL25 in fetal thymus colonization.[6] In the naturally occurring mutant mouse strain *plt*/*plt*, which is deficient for CCL21, or in mice deficient for CCR7, which is the receptor for CCL21, the number of fetal thymocytes was lower than that in normal mice until E14.5.[6] Similarly, mice deficient for CCR9, the receptor for CCL25, exhibited a 3-fold decrease in total thymocyte cellularity until E17.5.[7] On the other hand, it was shown that mice deficient for CXCL12 or its receptor CXCR4 were not defective in fetal thymus colonization.[8] These results suggested that fetal thymus colonization involved CCL21 and CCL25 rather than CXCL12. However, it is unclear whether the combination of CCL21 and CCL25 is sufficient for fetal thymus colonization or whether other chemotactic factors additionally play a role in fetal thymus colonization. It is also unclear how these 2 chemokines are involved in thymus colonization before and after thymus vascularization during embryogenesis. Furthermore, it is not known where, when, and how these chemokines are expressed in the thymic primordium and neighboring regions.

In the present study, we show that the coordination between CCL21/CCR7- and CCL25/CCR9-mediated chemokine signals is essential for guiding fetal thymus colonization before, but not after, thymus vascularization. By regulating prevascular fetal thymus colonization, the combination of these chemokine signals selectively regulates the first wave of T-cell development that includes the generation of canonical epidermal Vγ3$^+$ γδ T cells. The results also reveal an unexpected role of the parathyroid primordium in prevascular fetal thymus colonization. The expression of CCL21 in

From the Division of Experimental Immunology, Institute for Genome Research, University of Tokushima, Japan; the Department of Genetics, University of Georgia, Athens; the Laboratory of Mammalian Genes and Development, National Institute of Child Health and Human Development, National Institutes of Health, Bethesda, MD; the Department of Molecular Tumorgenetics and Immunogenetics, Max-Delbrück Center (MDC) for Molecular Medicine, Berlin, Germany; and JEOL, Akishima, Tokyo, Japan.

Submitted May 22, 2006; accepted June 12, 2006. Prepublished online as *Blood* First Edition Paper, June 29, 2006; DOI 10.1182/blood-2006-05-024190.

Supported by the MEXT (Ministry of Education, Culture, Sports, Science, and Technology) grants-in-aid for scientific research, the JSPS (Japanese Society for the Promotion of Science) core-to-core program, and the JSPS center-of-excellence program (Y.T.).

C.L. and Y.T. designed the study and wrote the paper; N.M. conceived the idea of parathyroid involvement; C.L. performed the majority of experiments; F.S. performed confocal microscopy analysis; C.L. and Y.L. performed flow cytometry analysis; S.K. performed electron microscopy analysis; Z.L. and N.M. provided Gcm2-deficient embryos; S.U. and P.L. provided CCR9-deficient mice; and M.L. provided CCR7-deficient mice.

The online version of this article contains a data supplement.

An Inside *Blood* analysis of this article appears at the front of this issue.

Reprints: Yousuke Takahama, Division of Experimental Immunology, Institute for Genome Research, University of Tokushima, Tokushima 770-8503, Japan; e-mail: takahama@genome.tokushima-u.ac.jp.

The publication costs of this article were defrayed in part by page charge payment. Therefore, and solely to indicate this fact, this article is hereby marked "advertisement" in accordance with 18 U.S.C. section 1734.

the third pharyngeal pouch region is neither localized at the thymic primordium nor controlled by the transcription factor Foxn1. Instead, CCL21 is expressed by neighboring parathyroid primordium and is controlled by the parathyroid-specifying transcription factor Gcm2. On the other hand, CCL25 is expressed by both parathyroid and thymic primordia, and is regulated in both Foxn1-dependent and Foxn1/Gcm2-independent manners. Thus, our results indicate that parathyroid and thymic primordia coordinate in guiding prevascular fetal thymus colonization, by providing spatially distinct expressions of CCL21 and CCL25.

Materials and methods

Mice

Mice deficient for CCR7,[9] CCR9,[10] and Gcm2[11] were described previously. CCR7- and Gcm2-deficient mice were originated on a 129 × C57BL/6 mixed background and backcrossed to C57BL/6 mice for at least 7 and 4 generations, respectively. CCR9-deficient mice were on a 129 × C57BL/6 mixed background. *nu*/*nu* mice crossed with Gcm2-deficient mice were of C57BL/6 background. C57BL/6 (B6), BALB/c, and BALB/c-*nu*/*nu* mice were obtained from SLC, Shizuoka, Japan. The day when a vaginal plug was first observed was designated as gestation day 0.5.

Bromodeoxyuridine labeling of fetal thymocytes in vivo

Pregnant mice were given intraperitoneal injections of 2 mg bromodeoxyuridine (BrdU). At 2 hours after the injection, fetal thymocytes were stained with FITC-labeled anti-BrdU monoclonal antibody (BD Pharmingen, San Diego, CA) and PE-labeled anti-CD45 antibody, and analyzed by flow cytometry.

Annexin V staining of fetal thymocytes

Fetal thymocytes were stained with PE-labeled annexin V (BD Pharmingen) according to the manufacturer's instructions.

Analysis of postnatal thymus immigration in vivo

Equal numbers of lineage (CD3, CD4, CD8, CD11b, CD11c, B220, Gr1, TER119, Thy1)–negative bone marrow cells were labeled with carboxyfluorescein succinimidyl ester (CFSE). Short-term thymus homing was analyzed as described.[12]

Analysis of fetal thymus attraction in vitro

Attraction of equal numbers of $CD45^+TER119^-FcR^-$ E14.5 fetal liver lymphoid progenitor cells was measured in a 24-hour culture as described.[6,13]

Fetal thymus organ culture

Organ culture of fetal thymus lobes was carried out as previously described.[13]

Preparation of epidermal cells

Epidermal cells were prepared as previously described,[14] with slight modification. Briefly, skin from the abdomen of newborn mice and from the ears of adult mice was digested with 0.25% Trypsin-EDTA for 60 and 30 minutes, respectively. Epidermal sheets were separated from dermal tissue and were mechanically dissociated for the preparation of single-cell suspensions of epidermal cells.

Multicolor confocal microscopy analysis

Immunofluorescence staining and confocal microscopy analysis of frozen sections and epidermal sheets were performed as previously described.[6,15-17] Monoclonal antibodies specific for mouse CCL21 and CCL25 were purchased from R&D Systems (Minneapolis, MN), rabbit antikeratin polyclonal antibody was from Dako (Carpinteria, CA), and FITC–anti-Vγ3 antibody (clone 536) was from BD Pharmingen.

Confocal images were acquired by TCS SP2 laser scanning microscopy equipped with argon and helium-neon lasers (Leica, Mannheim, Germany) and 40 ×/1.25-0.75 CS oil objectives. Imaging medium was obtained from Dako. Images were acquired using Leica confocal software version 2.0.

Multicolor flow cytometry analysis

Immunofluorescence staining and flow cytometry analysis of single-cell suspensions were performed as previously described.[6] CCR7 was detected with CCL19-Ig reagent kindly provided by Dr K. Hieshima (Kinki University, Osaka, Japan).[17] Anti-CCR9 monoclonal antibody was purchased from R&D Systems.

Scanning electron microscopy analysis of embryonic blood vessels

Normal mouse embryos were given injections of resin through the umbilical cord and the tissues were digested.[18] Images were visualized using a Hitachi S-800 electron microscope (Hitachinaka, Ibaraki, Japan).

Statistics

All values are expressed as means plus or minus standard errors. Statistical comparison was performed with the Student *t* test using StatView software.

Results

Defective colonization of fetal thymus primordium in mice lacking CCR7 and CCR9

We previously showed that neutralizing antibodies specific for CCL21 and CCL25 significantly inhibit the in vitro attraction of T-lymphoid progenitor cells to the fetal thymus rudiment, suggesting that CCL21 and CCL25 are involved in fetal thymus colonization.[6] In order to examine the role of CCL21 and CCL25 in fetal thymus colonization, we analyzed the numbers of fetal thymocytes in mice deficient for CCR7 (a receptor for CCL21) and/or CCR9 (a receptor for CCL25). As shown in Figure 1A and in agreement with previous reports,[6,7] mice deficient for either CCR7 or CCR9 had reduced numbers (30%-40% of normal number) of E14.5 fetal thymocytes. Strikingly, however, the reduction in fetal thymocyte number was marked (2% of normal number) in mice deficient for both CCR7 and CCR9 (Figure 1A).

The reduced number of E14.5 fetal thymocytes might be due to reduced thymus colonization by T-lymphoid progenitor cells and/or reduced expansion of thymocytes after thymus colonization. The number of leukocytes that colonized the third pharyngeal pouch–derived thymic primordium at E11.5 (the earliest stage at which fetal thymus colonization is detected in mouse embryogenesis[1]) was markedly reduced in CCR7/CCR9 double-deficient mice, as shown by the confocal microscopy analysis of embryonic sections (Figure 1B-C). The number of E14.5 fetal liver lymphoid progenitor cells attracted to normal fetal thymus rudiment was significantly reduced in CCR7/CCR9 double-deficient mice, as shown in the in vitro visualization analysis[6] (Figure 1D). Technical differences among direct cell-number determination (Figure 1A), 2-dimensional section analysis (Figure 1C), and the in vitro visualization analysis (Figure 1D) might have contributed to the different ratios of cell numbers obtained by these analyses. On the other hand, in vivo bromodeoxyuridine labeling and in vitro annexin V staining indicated that the frequencies of proliferating cells and apoptotic cells were not affected in E14.5 fetal thymocytes of CCR7/CCR9 double-deficient mice (Figure 2A-B). The expression of CCL21

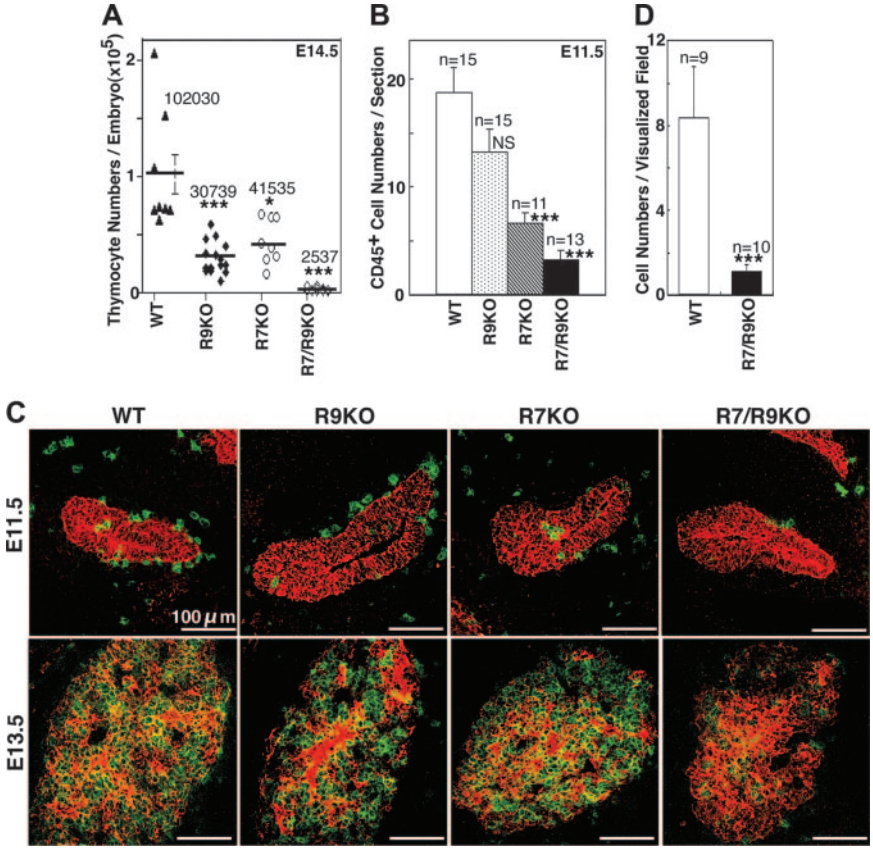

Figure 1. Fetal thymus colonization in CCR7/CCR9-deficient mice between E11.5 and E14.5. (A) Single-cell suspensions isolated from the fetal thymus of indicated mice (WT, wild-type; R9KO, CCR9-knockout; R7KO, CCR7-knockout; R7/R9KO, CCR7/CCR9-double-knockout) were stained for CD45. The frequency of $CD45^+$ cells was measured by flow cytometry. Thymocyte numbers were calculated from the frequency of $CD45^+$ cells and the total viable cell numbers identified by the trypan blue dye exclusion method. Symbols indicate thymocyte numbers in individual embryos, and bars indicate means plus or minus standard errors. Numbers indicate means. (B, C) Sagittal sections of frozen embryos from indicated mice were 2–color-stained for CD45 (Alexa 633; green in panel C) and keratin (FITC; red in panel C). Plotted in panel B are the means plus or minus standard errors of the numbers of $CD45^+$ cells in and attached to the third pharyngeal pouch that contains the thymic primordium. Representative images are shown in panel C, and the numbers of sections analyzed are indicated in panel B. (D) Number (means ± standard errors) of $CD45^+TER119^-FcR^-$ E14.5 fetal liver cells from indicated mice that were attracted to the deoxyguanosine-treated E14.5 B6 fetal thymus lobe in 1-day culture was determined as previously described.[6] $^*P < .05$; $^{***}P < .001$; NS, not significant.

and CCL25 as well as the stromal architecture identified by the generation of keratin 5 or keratin 8 single-positive thymic epithelial cells was not impaired in the fetal thymus of CCR7/CCR9 double-deficient mice (Figure S1, available on the *Blood* website; see the Supplemental Figure link at the top of the online article). These results indicate that the reduced number of E14.5 fetal thymocytes in CCR7/CCR9 double-deficient mice resulted from reduced thymus colonization by T-lymphoid progenitor cells rather

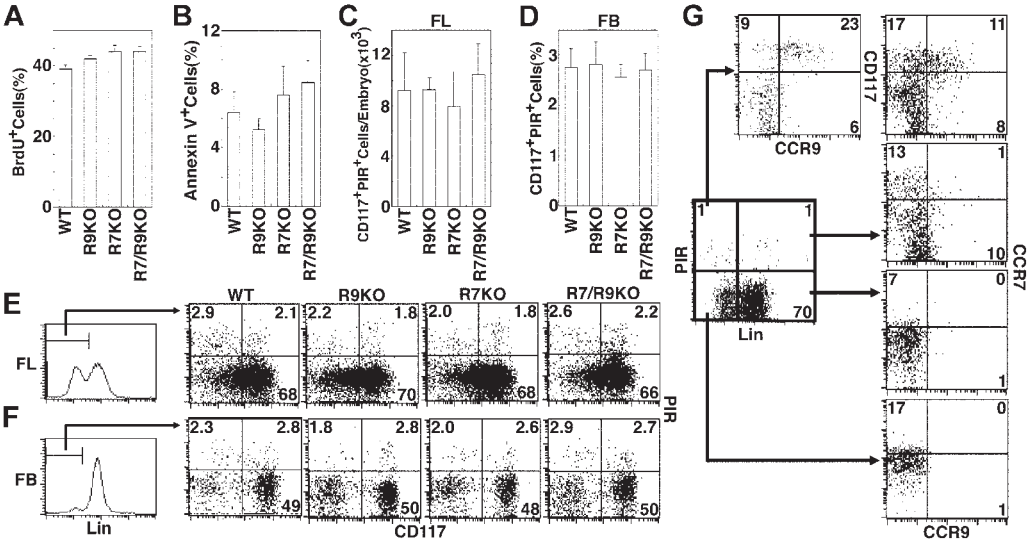

Figure 2. T-lymphoid progenitor cells in CCR7/CCR9-deficient embryos. (A) BrdU was pulsed for 2 hours to pregnant mice carrying E14.5 embryos, and the frequency of BrdU-incorporated cells in $CD45^+$ embryonic thymocytes was measured by flow cytometry. Bars indicate means plus or minus standard errors (n = 3 to 8), and the results show no significant difference. (B) Ex vivo E14.5 fetal thymocytes of indicated mice were stained with annexin V. Bars indicate means plus or minus standard errors (n = 4 to 10), and the results show no significant difference. (C-F) Fetal liver cells (FL, panels C and E) and fetal blood cells (FB, panels D and F) from E12.5 embryos of indicated mice were 3-color stained for Lin (TER119, B220, Gr-1, Thy1.2 and NK1.1), CD117, and PIR. Plotted in panels C and D are the means plus or minus standard errors (n = 3 to 7) of the number (FL, panel C) and the frequency (FB, panel D) of $Lin^-CD117^+PIR^+$ cells, and no significant difference was noted among the 4 groups. Representative flow cytometry profiles are shown in panels E and F. Histograms shown on the left indicate Lin expression profiles and the gates for Lin^- cells. Numbers with dot profiles of CD117 versus PIR in Lin^- cells indicate frequency within the boxes. (G) Fetal liver cells from E12.5 embryos of B6 mice were 4-color stained for Lin, PIR, CCR9, and either CD117 or CCR7. Representative flow cytometry profiles of Lin versus PIR (left, bold), CCR9 versus CD117 within Lin^-PIR^+ population (left, top), and CCR9 versus CCR7 within indicated Lin/PIR populations (right) from 3 independent measurements are indicated. Numbers indicate frequency within the boxes.

than reduced expansion of thymocytes after thymus colonization. These results also indicate that the combination of chemokine signals mediated by CCR7 and CCR9 plays a major role in the initial colonization of the fetal thymus primordium by T-lymphoid progenitor cells.

The reduced fetal thymus colonization in CCR7/CCR9 double-deficient mice did not coincide with the accumulation of T-lymphoid progenitor cells, which were identified as $Lin^-CD117^+PIR^+$,[19] in E12.5 fetal liver (Figure 2C,E). In addition, $Lin^-CD117^+PIR^+$ T-lymphoid progenitor cells in fetal blood were detected at normal levels and not reduced in CCR7/CCR9 double-deficient E12.5 embryos (Figure 2D,F). These results indicate that the reduced fetal thymus colonization in CCR7/CCR9 double-deficient mice is due to impaired migration of T-lymphoid progenitor cells from the circulation to the thymus, and not to impaired emigration of T-lymphoid progenitor cells from hematopoietic organs, such as fetal liver, to the circulation. It should also be noted that the $Lin^-CD117^+PIR^+$ fetal liver cells in normal embryos were predominantly $CCR9^+$ and the $Lin^-CCR9^+PIR^+$ fetal liver cells were mostly $CCR7^+$ (Figure 2G), indicating that $Lin^-CD117^+PIR^+$ T-lymphoid progenitor cells generated in fetal liver are highly enriched for cells that express both CCR7 and CCR9.

Role of CCR7 and CCR9 in prevascular but not postvascular fetal thymus seeding

The reduction in the number of thymocytes present in CCR7/CCR9 double-deficient fetal mice was reversed during subsequent embryogenesis, as thymocyte numbers in CCR7/CCR9 double-deficient mice by postnatal day 1 (P1) were equal to those in normal mice (Figure 3A). Accordingly, whereas thymocyte development in CCR7/CCR9 double-deficient mice was delayed during embryogenesis, as shown by the reduced generation of $CD4^+CD8^+$ cells at E16.5, thymocyte development in CCR7/CCR9 double-deficient mice was normal at day P1 (Figure 3B). The recovery of thymocyte development was partially, but not entirely, attributed to the compensatory proliferation of a small number of thymocytes that colonized CCR7/CCR9 double-deficient thymi by E14.5, because (1) in vitro organ culture of fetal thymus lobes showed that the number of thymocytes in the thymus isolated at E14.5 from CCR7/CCR9 double-deficient mice was partially recovered but remained small even after 6 days of culture (34% of normal number after the culture, as shown in Figure 3C, and 2% of normal number before the culture, as shown in Figure 1A), and (2) in vivo bromodeoxyuridine labeling of E14.5 and E16.5 fetal thymocytes showed that the frequency of proliferating cells was not significantly elevated compared with the normal level in CCR7/CCR9 double-deficient mice (Figure 2A and Figure 3D). It was therefore reasoned that the recovery of thymocyte number in CCR7/CCR9 double-deficient mice during late embryogenesis was due to the combination of thymocyte proliferation and subsequent seeding of T-lymphoid progenitor cells at and after E14.5, and that this late seeding of the thymus was mediated by a mechanism that was independent of CCR7 and CCR9. The embryonic timing of such CCR7/CCR9-independent seeding coincided with the thymus vascularization (Figure 3E). Indeed, vasculature development in the embryonic thymus was detected at and after E15.5 (Figure

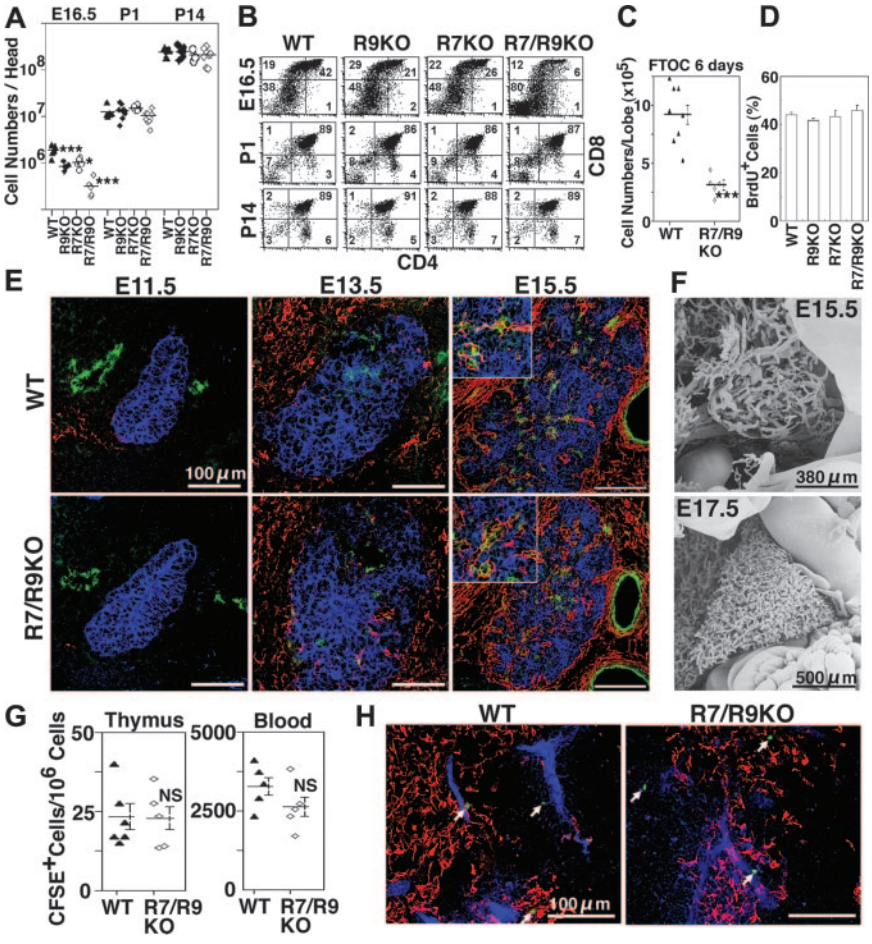

Figure 3. Postvascular thymus colonization in CCR7/CCR9-deficient mice. (A) Numbers of thymocytes from indicated mice at E16.5, postnatal day 1 (P1), and P14 are plotted. (B) Two-color flow cytometry analysis of indicated thymocytes for CD4 and CD8. Numbers indicate the frequency of cells in each quadrant. (C) E14.5 fetal thymus lobes were organ-cultured, and thymocyte numbers were measured at day 6 of culture. (D) BrdU was pulsed for 2 hours to pregnant mice carrying E16.5 embryos, and the frequency (means ± SE) of BrdU-incorporated embryonic thymocytes was measured by flow cytometry. (E) Frozen sections of indicated embryos were 3-color stained for endothelial CD31 (green, Alexa 568), mesenchymal ER-TR7 (red, Alexa 633), and keratin (blue, FITC). Higher magnification of the vasculatures is shown in the insets. (F) Scanning electron microscopy images of the vascular architecture in normal mouse embryos at the indicated gestational age. Embryos were intravenously microinjected with resin, and the tissues were digested, as described in "Materials and methods." (G, H) Equal numbers of lineage-negative bone marrow cells from indicated mice were labeled with CFSE and intravenously administered into adult wild-type mice. On day 2 after the administration, the number of $CFSE^+$ cells in thymocytes and blood leukocytes was measured by flow cytometry (panel G), and frozen sections of the thymus were analyzed for migrated $CFSE^+$ cells (green), $CD31^+$ endothelial cells (blue, Alexa 568), and $ER\text{-}TR5^+$ medullary thymic epithelial cells (red, Alexa 633) (panel H). $^*P < .05$; $^{***}P < .001$; NS, not significant.

3E-F), in both normal mice and CCR7/CCR9 double-deficient mice (Figure 3E). It was also shown that bone marrow progenitor cells isolated from CCR7/CCR9 double-deficient mice were capable of entering the postnatal thymus (Figure 3G-H), into which the entry of T-lymphoid progenitor cells is mediated by the vasculature enriched at the cortico-medullary junction[20] (also shown in Figure 3H). Thus, chemokine signals mediated by CCR7 and CCR9 are essential for fetal thymus seeding before, but not after, vascularization of the thymus.

Distinct localization of CCL21 and CCL25 in third pharyngeal pouch region

We then addressed how the 2 sets of chemokine signals via CCL21/CCR7 and CCL25/CCR9 cooperate to attract T-lymphoid progenitor cells to the fetal thymus. As was previously reported[5,6] and as is shown in Figure 4A,C, CCL21 protein was prominently expressed in the third pharyngeal pouch region, which contained the fetal thymus primordium, at E11.5. The prominent expression of CCL21 in the third pharyngeal pouch region was detected even earlier at E10.5 (Figure S1). On the other hand, the expression of CCL25 protein in the third pharyngeal pouch region was pronounced at E13.5 and faintly detectable at E11.5[6] (Figure 4E,G). Interestingly, CCL21 and CCL25 proteins were differently localized within the third pharyngeal pouch region; CCL21 was exclusively localized in an area at the dorsal-anterior aspect (Figure 4A,C), whereas CCL25 was detected in both dorsal-anterior and ventral-posterior areas (Figure 4E,G).

Foxn1 regulation of CCL25 but not CCL21 in third pharyngeal pouch region

As the third pharyngeal pouch gives rise to the thymus at the ventral-posterior domain and the parathyroid gland at the dorsal-anterior domain,[21] it was interesting to determine how the expression of the differently localized chemokines was regulated by transcriptional factors Foxn1 and Gcm2 that are essential for the development of the thymus[22,23] and the parathyroid,[11,24] respectively. In Foxn1-deficient *nu/nu* mice, fetal thymus development, including thymocyte seeding, is severely defective,[21,23,25] which was apparent at and after E13.5 (Figure 4K-L,R). CCL25 expression in the third pharyngeal pouch region was lower in *nu/nu* mice than in normal mice (Figure 4E-H,O-P). The defect in CCL25 expression was obvious at the ventral-posterior domain of the thymic primordium, whereas the expression of CCL25 in the dorsal-anterior domain of the third pharyngeal pouch region was low but detectable in *nu/nu* mice (Figure 4F,H,P). Interestingly, the prominent expression of CCL21 in the dorsal-anterior domain of the third pharyngeal pouch region was not reduced in *nu/nu* mice at E11.5 or E13.5 (Figure 4A-D). Accordingly, the initial attraction of leukocytes to the third pharyngeal pouch region at E11.5 was not impaired in *nu/nu* mice (Figure 4I-J,Q). Thus, CCL21 is expressed in the dorsal-anterior domain of the third pharyngeal pouch region independent of Foxn1, whereas CCL25 is expressed in both the Foxn1-dependent ventral-posterior domain and the Foxn1-independent dorsal-anterior domain of the third pharyngeal pouch region.

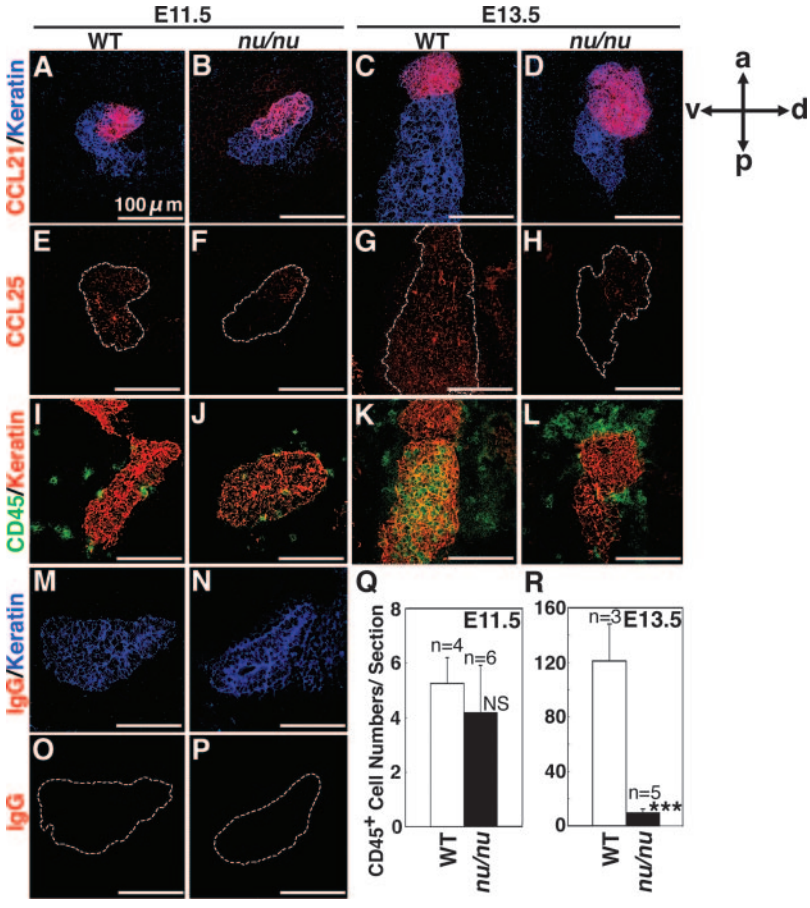

Figure 4. Chemokine expression and fetal thymus colonization in Foxn1-deficient mice. Sagittal sections of frozen embryos from indicated mice of BALB/c background were 2-color stained for CCL21 (Alexa 633, red) and keratin (FITC, blue) (A-D), CCL25 (Alexa 633, red) and keratin (areas surrounded by dashed lines indicate keratin-positive areas) (E-H), or CD45 (Alexa 633, green) and keratin (FITC, red) (I-L). Control IgG staining shows the specificity of CCL21 and CCL25 signals (M-P). Anterior-posterior (a-p) and dorsal-ventral (d-v) orientation of the images is indicated. The means plus or minus standard errors of the numbers of $CD45^+$ cells in and attached to the third pharyngeal pouch region that contains the thymic primordium are shown in panels Q and R. ***$P < .001$; NS, not significant.

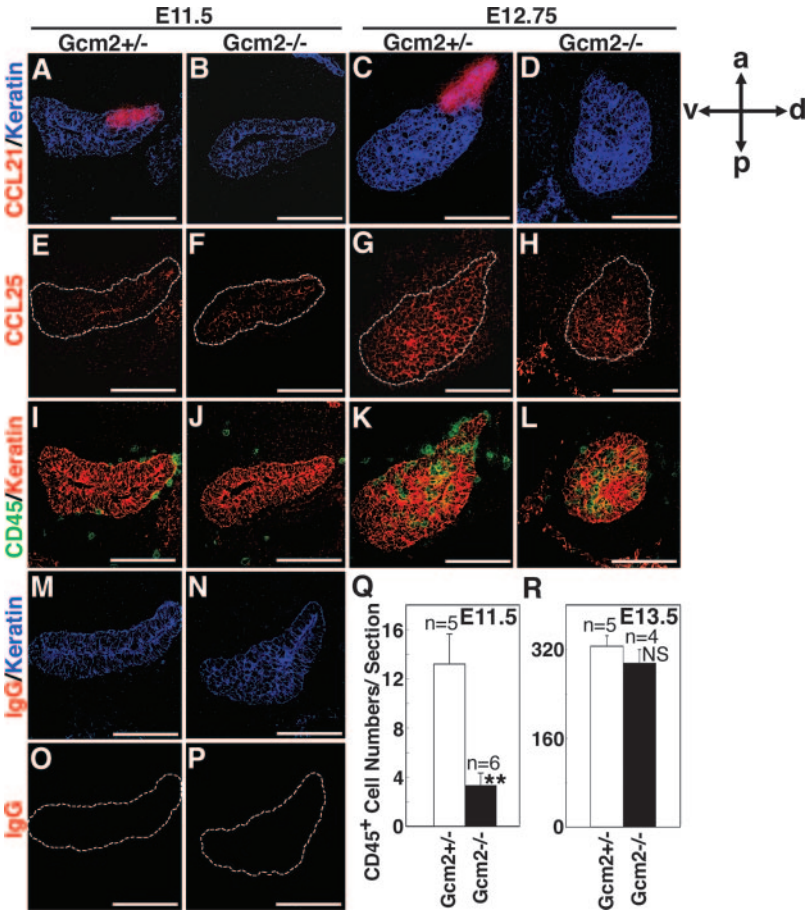

Figure 5. Chemokine expression and fetal thymus colonization in Gcm2-deficient mice. Sagittal sections of frozen embryos from indicated mice were analyzed as in Figure 4. $^{**}P < .005$; NS, not significant. Scale bars indicate 100 μm.

Gcm2-dependent expression of CCL21 but not CCL25 in third pharyngeal pouch region

The dorsal-anterior aspect of the third pharyngeal pouch gives rise to the parathyroid gland, which is essentially dependent on the transcriptional factor Gcm2.[11,24] We found that the expression of CCL21 in the developing third pharyngeal pouch region was undetectable in Gcm2-deficient mice (Figure 5A-D), whereas the expression of CCL25 in the thymic primordium was not impaired in Gcm2-deficient mice (Figure 5E-H,O-P). Accordingly, the initial phase of leukocyte attraction to the third pharyngeal pouch region at E11.5 was significantly reduced in Gcm2-deficient mice (Figure 5I-J,Q), in agreement with the E11.5 phenotype of CCR7-deficient mice expressing CCL25 and CCR9 (Figure 1A-B). Nonetheless, the number of thymocytes that were subsequently accumulated within the thymic primordium was not significantly reduced in Gcm2-deficient mice (Figure 5K-L,R), possibly reflecting the combination of CCL25-mediated recruitment of T-lymphoid progenitor cells and intrathymic compensatory proliferation of colonized cells. Fetal thymus colonization in Gcm2-deficient mice seemed less severe than that in CCR7-deficient mice (Figures 1 and 5), suggesting that an undetectable level of CCL21 may be expressed in the third pharyngeal pouch region of Gcm2-deficient embryos. These results indicate that CCL21 localized at the dorsal-anterior domain of the third pharyngeal pouch region is expressed by the parathyroid primordium under the control of Gcm2 and not Foxn1, and this Gcm2-dependent CCL21 expression contributes significantly to the initial attraction of hematopoietic progenitor cells to the third pharyngeal pouch region.

Expression of CCL21 and CCL25 in third pharyngeal pouch region in mice lacking Foxn1 and Gcm2

As shown in Figure 4, CCL25 was expressed both in the Foxn1-dependent ventral-posterior domain and in the Foxn1-independent dorsal-anterior domain of the third pharyngeal pouch region. Although the CCL25 expression was not clearly impaired in Gcm2-deficient mice (Figure 5), it was interesting to address whether the dorsal-anterior expression of CCL25 independent of Foxn1 might be dependent on Gcm2. To this end, we examined chemokine expression and fetal thymus colonization in Gcm2-deficient *nu/nu* mice (Figure 6). As speculated from the phenotypes of Gcm2-deficient mice and Foxn1-deficient *nu/nu* mice, CCL21 expression in the third pharyngeal pouch region was undetectable and leukocyte recruitment to the thymic region was impaired in E11.5 embryos of Gcm2-deficient *nu/nu* mice (Figure 6A-D,I-L). We found that the expression of CCL25 in the third pharyngeal pouch region was reduced but detectable in Gcm2-deficient *nu/nu* mice (Figure 6E-H,Q-T). The localization and expression levels of CCL25 in the third pharyngeal pouch region were comparable between Gcm2-deficient *nu/nu* mice and *nu/nu* mice (Figure 6G-H,S-T). Thus, the expression of CCL25 in the third pharyngeal pouch region is induced even in the absence of Foxn1 and Gcm2, and Foxn1 enhances CCL25 expression in the thymic primordium.

Defective generation of Vγ3$^+$ T cells in mice lacking CCR7 and CCR9

Finally, we examined how the chemokine-mediated prevascular colonization of the fetal thymus may contribute to the formation

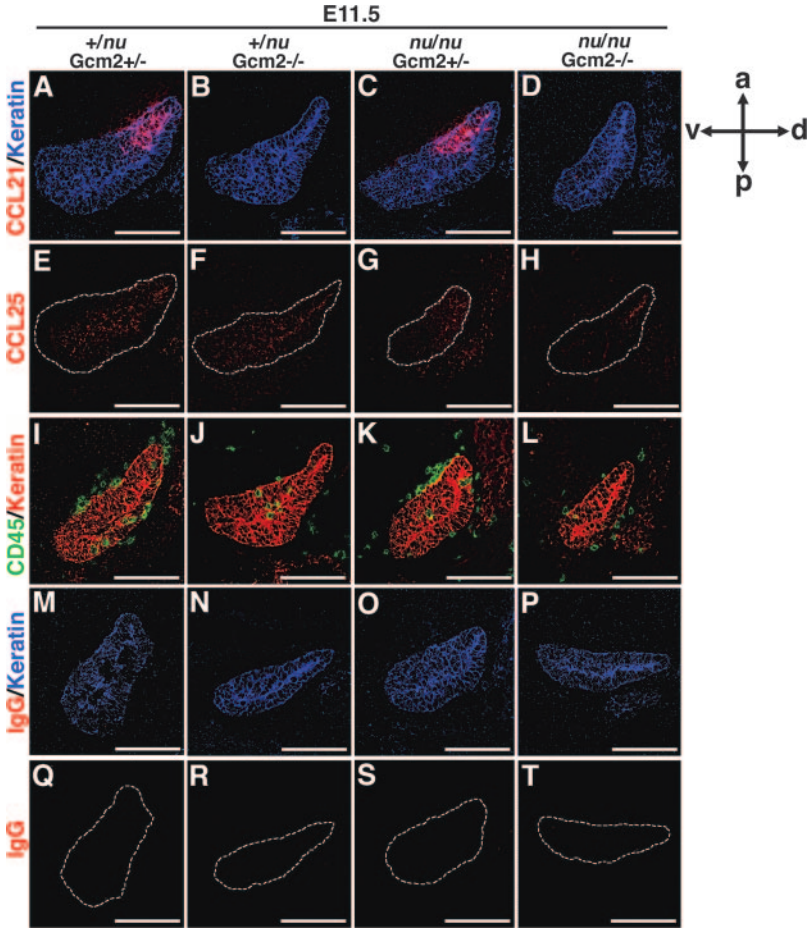

Figure 6. Chemokine expression and fetal thymus colonization in Foxn1/Gcm2-deficient mice. Sagittal sections of frozen embryos from indicated mice were analyzed as in Figure 4. Scale bars indicate 100 μm.

of the postnatal immune system. It was shown that dendritic epidermal Vγ3$^+$ T cells, which critically modulate innate immune surveillance and homeostasis in the skin,[26-29] are derived from the first wave of T-cell development in the fetal thymus.[15,30] It was speculated that the chemokine-mediated prevascular colonization of the fetal thymus might play a role in the development of canonical γδ T cells in the skin. As shown in Figure 7, the generation of Vγ3$^+$ T cells, which represented the majority of γδ T cells in the fetal thymus at E15.5 (Figure 7A,C) and the postnatal skin at P7 (Figure 7B-D), was significantly reduced in CCR7/CCR9 double-deficient mice (1% and 14% of normal numbers in the E15.5 fetal thymus and the P7 skin, respectively). Unlike the reduction of prenatal Vγ3$^+$ thymocyte generation, the numbers of systemically distributing Vγ2$^+$ thymocytes at E15.5 and P7 were not impaired (Figure 7A), suggesting that the first-wave skin-homing Vγ3$^+$ T cells are selectively defective in CCR7/CCR9 double-deficient mice. In the skin of CCR7/CCR9 double-deficient newborn mice, the generation of MHC class II$^+$ Langerhans cells was not reduced unlike Vγ3$^+$ T cells (Figure 7D), suggesting that the skin homing of hematopoietic cells is not generally impaired in mice lacking CCR7 and CCR9. Nevertheless, the reduced number of epidermal Vγ3$^+$ T cells in CCR7/CCR9 double-deficient newborn mice was restored to normal numbers at 7 to 9 weeks of age (Figure 7B-C). Thus, the defective colonization of the prevascular thymus in CCR7/CCR9 double-deficient mice was followed by the defective generation of Vγ3$^+$ T cells in the prenatal thymus and the postnatal skin in newborn mice.

Discussion

Colonization of the thymus begins during embryonic development and before the thymus is vascularized. It has been suggested that chemotactic factors are involved in the attraction of T-lymphoid progenitor cells toward the fetal thymus, but how T-lymphoid progenitor cells are attracted to the fetal thymus at the pre- and postvascular stages has remained unclear. The present results show that mice deficient for both CCR7 and CCR9 are defective in fetal thymus colonization before, but not after, vascularization of the thymus. These results reveal that the combination of chemokine signals mediated by CCR7 and CCR9 is essential for early fetal thymus colonization at the prevascular stage and that these chemokine signals are not needed for the postvascular stage of perinatal and postnatal thymus seeding.

Our results show that CCL25, a CCR9 ligand, is expressed both by the Foxn1-dependent ventral-posterior domain and by the Foxn1-independent dorsal-anterior domain of the third pharyngeal pouch region, whereas CCL21, a CCR7 ligand, is expressed in the third pharyngeal pouch region exclusively by the Gcm2-dependent and Foxn1-independent dorsal-anterior domain. Although the roles of CCL21 and CCL25 in various aspects of development and function of immune cells have been reported,[9,10,31,32] their combinatorial role in fetal thymus colonization, as described in this study, is, to our knowledge, the earliest function of these 2 chemokines in ontogeny. More importantly, the coordination between these 2 chemokines that are expressed in a spatially different manner offers

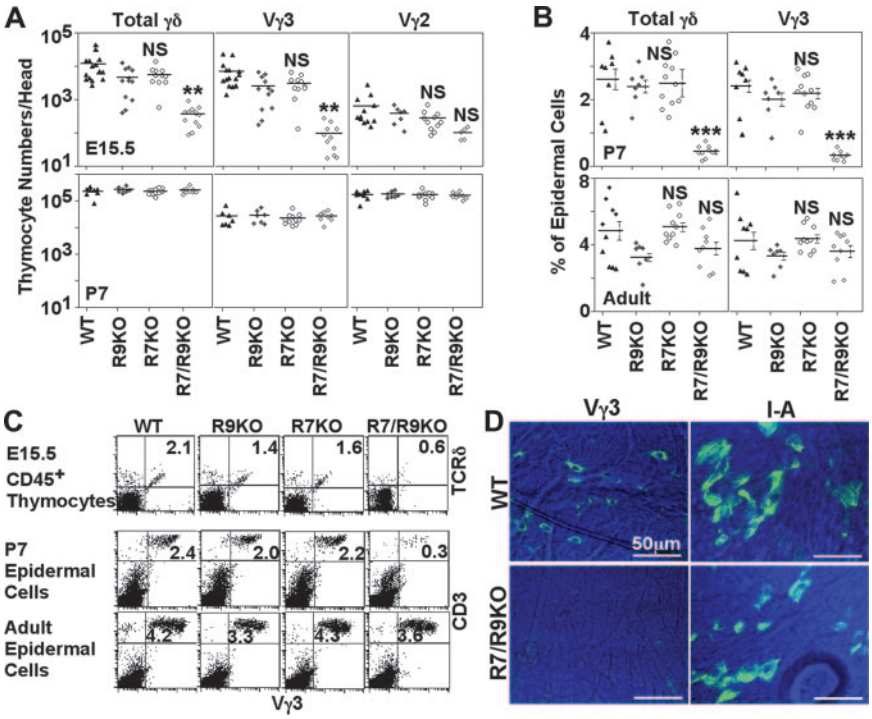

Figure 7. Generation of Vγ3$^+$ T cells in the thymus and skin of CCR7/CCR9-deficient mice. (A) E15.5 fetal thymocytes (top panels) and 7-day-old newborn thymocytes (P7, bottom panels) isolated from indicated mice were stained for CD45 and either one of TCR-Cδ (for total γδ), Vγ3, or Vγ2. Cell number of indicated population was calculated from total viable thymocyte number and the frequency of that population. Symbols indicate the number of indicated thymocyte populations in individual mice, and bars indicate their means. (B) Epidermal cells isolated from abdomen skin of 7-day-old (P7) newborn mice or ear skin of 7- to 9-week-old adult mice were stained for TCR-Cδ or Vγ3. Symbols indicate the frequency of indicated cell populations within the total viable epidermal cells, and bars indicate means plus or minus standard errors. (C) Representative flow cytometry profiles of indicated thymocytes and epidermal cells are shown. Numbers in the dot plots indicate the frequency of cells within the quadrant. (D) Representative immunofluorescence images of 7-day-old epidermal sheets of Vγ3$^+$ T cells or I-A$^+$ Langerhans cells were visualized (FITC signals in green) in epidermal sheets (background signals in blue) from indicated mice. Images were obtained using a 63 ×/1.40-0.60 oil objective. $^{**}P < .005$; $^{***}P < .001$; NS, not significant.

a novel insight into the mechanisms underlying the colonization of the fetal thymus by T-lymphoid progenitor cells at the prevascular stage, predicting a vasculature-independent yet orientation-specific guidance of T-lymphoid progenitor cells toward the thymus by the sequential deposition of chemotactic molecules. Indeed, the data presented here suggest the directional migration of T-lymphoid progenitor cells into the prevascular fetal thymus from the dorsal-anterior edge of the thymic primordium, the edge adjacent to the CCL21-expressing parathyroid primordium (Figure 4K,L).

Our results further indicate the involvement of the Gcm2-dependent parathyroid in thymus development, revealing a previously unidentified role of this endocrine organ in immune system development. At the E11.5 prevascular stage, the defect in attracting T-lymphoid progenitor cells to the vicinity of the thymic primordium was more pronounced in CCR7-deficient mice than in CCR9-deficient mice (Figure 1), in agreement with the more prominent expression of CCL21 than CCL25 in the third pharyngeal pouch region at E11.5[6] and with the more severe reduction of leukocyte colonization at E11.5 in Gcm2-deficient (and CCL21-defective in the third pharyngeal pouch region) mice than in Foxn1-deficient (and CCL25-defective only in the thymus primordium) *nu*/*nu* mice (Figures 4 and 5). It is possible that the earlier expression of CCL21 by the Gcm2-dependent parathyroid primordium and the later increase of CCL25 expression by the Foxn1-dependent thymic primordium sequentially guide the prevascular fetal thymus colonization.

Unlike CCR7 and CCR9 double deficiency, our results also show that selective deficiency of either CCR7 or CCR9 only partially reduces, but does not nullify, the number of fetal thymocytes at E14.5. Similarly, fetal thymus colonization in CCL21-deficient *plt*/*plt* mice or Gcm2-deficient (and CCL21-defective in the parathyroid primordium) mice was deficient only in the early stages of embryogenesis and was restored during late embryogenesis, as shown in Liu et al[6] and in this study. Thus, the recruitment of T-lymphoid progenitor cells to the thymic primordium is unlikely to be solely controlled by the tandem coordination between the 2 chemokines, CCL21 and CCL25. Rather, it is possible that either CCL21 or CCL25 is partially capable of mediating prevascular thymus colonization. Alternatively, but not mutually exclusively, it is also possible that prevascular thymus colonization may be additionally controlled by factors other than these 2 chemokines, including adhesion molecules and/or interstitial flow, which can partially compensate for the absence of either one of the chemokine signals.

We found that vasculature development in the embryonic thymus was detected as early as E15.5, and this timing coincided with the restoration of thymocyte numbers in CCR7/CCR9 double-deficient mice. The results also show that T-lymphoid progenitor cells from CCR7/CCR9 double-deficient mice were normally capable of entering the adult thymus, which is well vascularized. These results suggest that the chemokine signals mediated by CCL21/CCR7 and CCL25/CCR9 are not needed for thymus seeding by T-lymphoid progenitor cells after thymus vascularization. It was previously shown that in adult mice, T-lymphoid progenitor cells enter the postnatal thymus through the vasculature enriched at the cortico-medullary junction,[20] and this postnatal thymus seeding is regulated by the adhesive interaction between P-selectin expressed by endothelial cells and its ligand PSGL-1 expressed by T-lymphoid progenitor cells.[12] Thus, seeding of the thymus is likely mediated by at least 2 different mechanisms: (1) the CCL21/CCL25-dependent and vasculature-independent mechanism, which is operational during fetal thymus colonization before thymus vascularization, and (2) the CCL21/CCL25-independent and vasculature-dependent mechanism, which is operational in the vascularized thymus during late embryogenesis and after birth, and is regulated by the P-selectin–mediated adhesive cell-cell interaction. It is still unclear whether chemokines other than CCL21 and CCL25 may be involved in the latter seeding mechanism in the vascularized thymus.

Finally, the present results show that the defective thymus colonization in CCR7/CCR9 double-deficient mice was followed by the defective generation of Vγ3$^+$ T cells in the prenatal thymus and the neonatal skin. It was shown that epidermal γδ T cells expressing the canonical Vγ3$^+$ T-cell receptor are an essential

component of innate immune surveillance and homeostasis in the skin,[26-29] and are derived from the first wave of T-cell development in the fetal thymus.[15,30] However, the reduced number of epidermal $V\gamma3^+$ T cells in CCR7/CCR9 double-deficient newborn mice was restored to normal numbers during growth to adulthood. This restoration may be due to the in situ proliferation of the small number of $V\gamma3^+$ T cells that home to the skin, as previously noted,[16,33] and/or the additional supply of late appearing $V\gamma3^+$ thymocytes from the newborn thymus. Nonetheless, it was speculated that the epidermal $V\gamma3^+$ T cells might be particularly important soon after birth before the full acquisition of pathogen-specific systemic responses.[34] Thus, the loss of epidermal $V\gamma3^+$ T cells in newborn CCR7/CCR9 double-deficient mice may impair the first line of defense against infectious pathogens attacking the surface of infants.

Unlike $V\gamma3^+$ fetal thymocytes, the $V\gamma2^+$ thymocytes that develop subsequently were not defective in CCR7/CCR9 double-deficient perinatal mice, suggesting that the skin-homing $V\gamma3^+$ T cells are selectively defective in CCR7/CCR9 double-deficient mice. We think that the defective generation of $V\gamma3^+$ T cells in the skin of CCR7/CCR9 double-deficient mice is largely due to the defective generation of first-wave T cells in the thymus rather than the defective homing of $V\gamma3^+$ T cells from the thymus to the skin, because (1) the number of $V\gamma3^+$ T cells in CCR7/CCR9 double-deficient mice was severely reduced in the fetal thymus (more severe than the reduction in newborn skin), (2) the distribution of Langerhans cells in the skin of CCR7/CCR9 double-deficient mice was not affected, suggesting that skin homing of hematopoietic cells is not generally impaired in the absence of CCR7 and CCR9, and (3) skin homing of $V\gamma3^+$ T cells was shown to be regulated by other molecules such as CCR10/CCL27 and integrin αE.[35,36] Together, we conclude that the CCL21- and CCL25-mediated prevascular colonization of the fetal thymus plays a critical role in the first wave of T-cell development, including the development of postnatal epidermal $V\gamma3^+$ T cells.

In summary, we have identified 2 major chemokine attractants required specifically for colonization of the fetal thymus prior to vascularization, and have demonstrated a surprising and hitherto unknown role of the developing parathyroid in immune system development.

Acknowledgments

We thank Drs E. Richie and A. Venables for sharing their unpublished data on fetal thymus vascularization, Dr K. Hieshima for the CCL19-Ig reagent, and Drs T. Ushiki, N. Iwanami, T. Nitta, and A. Singer for reading the manuscript.

References

1. Moore MAS, Owen JJT. Experimental studies on the development of the thymus. J Exp Med. 1967; 126:715-726.
2. Haynes BF, Heinly CS. Early human T cell development: analysis of the human thymus at the time of initial entry of hematopoietic stem cells into the fetal thymic microenvironment. J Exp Med. 1995; 181:1445-1458.
3. Fontaine-Perus JC, Calman FM, Kaplan C, Le Douarin NM. Seeding of the 10-day mouse embryo thymic rudiment by lymphocyte precursors in vitro. J. Immunol. 1981;126:2310-2316.
4. Wilkinson B, Owen JJT, Jenkinson EJ. Factors regulating stem cell recruitment to the fetal thymus. J Immunol. 1999;162:3873-3881.
5. Bleul CC, Boehm T. Chemokines define distinct microenvironments in the developing thymus. Eur J Immunol. 2000;30:3371-3379.
6. Liu C, Ueno T, Kuse S, et al. The role of CCL21 in recruitment of T precursor cells to fetal thymus. Blood. 2005;105:31-39.
7. Wurbel MA, Malissen M, Guy-Grand D, et al. Mice lacking the CCR9 CC-chemokine receptor show a mild impairment of early T- and B-cell development and a reduction in T-cell receptor $\gamma\delta^+$ gut intraepithelial lymphocytes. Blood. 2001;98: 2626-2632.
8. Ara T, Itoi M, Kawabata K, et al. A role of CXC chemokine ligand 12/stromal cell-derived factor-1/pre-B cell growth stimulating factor and its receptor CXCR4 in fetal and adult T cell development in vivo. J Immunol. 2003;170:4649-4655.
9. Forster R, Schubel A, Breitfeld D, et al. CCR7 coordinates the primary immune response by establishing functional microenvironments in secondary lymphoid organs. Cell. 1999;99:23-33.
10. Uehara S, Grinberg A, Farber JM, Love PE. A role for CCR9 in T lymphocyte development and migration. J Immunol. 2002;168:2811-2819.
11. Gunther T, Chen ZF, Kim J, et al. Genetic ablation of parathyroid glands reveals another source of parathyroid hormone. Nature. 2000;406:199-203.
12. Rossi FM, Corbel SY, Merzaban JS, et al. Recruitment of adult thymic progenitors is regulated by P-selectin and its ligand PSGL-1. Nature Immunol. 2005;6:626-634.
13. Ueno T, Liu C, Nitta T, Takahama Y. The development of T lymphocytes in mouse fetal thymus organ culture. Methods Mol Biol. 2005;290: 117-134.
14. Tamaki K, Stingl G, Gullino M, Sachs DH, Katz SI. Ia antigens in mouse skin are predominantly expressed on Langerhans cells. J Immunol. 1979;123:784-787.
15. Havran WL, Allison JP. Origin of Thy-1^+ dendritic epidermal cells of adult mice from fetal thymic precursors. Nature. 1990;344:68-70.
16. Kawai K, Suzuki H, Tomiyama K, Minagawa M, Mak TW, Ohashi PS. Requirement of the IL-2 receptor β chain for the development of Vγ3 dendritic epidermal T cells. J Invest Dermatology. 1998;110:961-965.
17. Ueno T, Saito F, Kuse S, et al. CCR7 signals are essential for cortex-to-medulla migration of developing thymocytes. J Exp Med. 2004;200: 493-505.
18. Kondo S. Microinjection methods for visualization of the vascular architecture of the mouse embryo for light and scanning electron microscopy. J Electron Microsc. 1998;47:101-113.
19. Masuda K, Kubagawa H, Ikawa T, et al. Prethymic T-cell development defined by the expression of paired immunoglobulin-like receptors. EMBO J. 2005;24:4052-4060.
20. Lind EF, Prockop SE, Porritt HE, Petrie HT. Mapping precursor movement through the postnatal thymus reveals specific microenvironments supporting defined stages of early lymphoid development. J Exp Med. 2001;194:127-134.
21. Cordier AC, Haumont SM. Development of thymus, parathyroids, and ultimobranchial bodies in NMRI and nude mice. Am J Anat. 1980;157: 227-263.
22. Nehls M, Pfeifer D, Schorpp M, Hedrich H, Boehm T. New member of the winged-helix protein family disrupted in mouse and rat nude mutations. Nature. 1994;372:103-107.
23. Nehls M, Kyewski B, Messerle M, et al. Two genetically separable steps in the differentiation of thymic epithelium. Science. 1996;272:886-889.
24. Gordon J, Bennett AR, Blackburn CC, Manley NR. Gcm2 and Foxn1 mark early parathyroid- and thymus-specific domains in the developing third pharyngeal pouch. Mech Dev. 2001;103: 141-143.
25. Itoi M, Kawamoto H, Katsura Y, Amagai T. Two distinct steps of immigration of hematopoietic progenitors into the early thymus anlage. Int Immunol. 2001;13:1203-1211.
26. Girardi M, Oppenheim DE, Steele CR, et al. Regulation of cutaneous malignancy by $\gamma\delta$ T cells. Science. 2001;294:605-609.
27. Girardi M, Lewis J, Glusac E, et al. Resident skin-specific $\gamma\delta$ T cells provide local, nonredundant regulation of cutaneous inflammation. J Exp Med. 2002;195:855-867.
28. Jameson J, Ugarte K, Chen N, et al. A role for skin gammadelta T cells in wound repair. Science. 2002;296:747-749.
29. Sharp LL, Jameson JM, Cauvi G, Havran WL. Dendritic epidermal T cells regulate skin homeostasis through local production of insulin-like growth factor 1. Nature Immunol. 2005;6:73-79.
30. Ikuta K, Kina T, MacNeil I, et al. A developmental switch in thymic lymphocyte maturation potential occurs at the level of hematopoietic stem cells. Cell. 1990;62:863-874.
31. Weninger W, von Andrian UH. Chemokine regulation of naive T cell traffic in health and disease. Semin Immunol. 2003;15:257-270.
32. Kunkel EJ, Campbell DJ, Butcher EC. Chemokines in lymphocyte trafficking and intestinal immunity. Microcirculation. 2003;10:313-323.
33. Payer E, Elbe A, Stingl G. Circulating $CD3^+$/T cell receptor $V\gamma3^+$ fetal murine thymocytes home to the skin and give rise to proliferating dendritic epidermal T cell. J Immunol. 1991;146:2536-2543.
34. Hayday A, Tigelaar R. Immunoregulation in the tissues by $\gamma\delta$ T cells. Nature Rev Immunol. 2003; 3:233-242.
35. Schon MP, Schon M, Parker CM, Williams IR. Dendritic epidermal T cells are diminished in integrin αE (CD103)-deficient mice. J Invest Dermatol. 2002;119:190-193.
36. Xiong N, Kang C, Raulet DH. Positive selection of dendritic epidermal $\gamma\delta$ T cell precursors in the fetal thymus determines expression of skin-homing receptors. Immunity. 2004;21:121-131.